






Original Article


## Stable isotopes and chloride ion of precipitation events in the northeastern Tibetan Plateau, China


CUI Bu-li<sup>1,2,3\*</sup>  <https://orcid.org/0000-0002-0852-4947>;  e-mail: cuibuli@163.com


LI Dong-sheng<sup>2</sup>  <https://orcid.org/0000-0002-5135-0778>; e-mail: dongshengli7@163.com

JIANG Bao-fu<sup>2</sup>  <https://orcid.org/0000-0001-6835-3732>; e-mail: jiangbaofu523@126.com

WANG Ying<sup>2</sup>  <https://orcid.org/0000-0003-4290-7500>; e-mail: xiyan960211@163.com

WANG Ya-xuan<sup>2</sup>  <https://orcid.org/0000-0002-4506-9744>; e-mail: wangyaxuan09@163.com

WANG Long-sheng<sup>2</sup>  <https://orcid.org/0000-0002-0308-2211>; e-mail: 52wls@163.com

LI Xiao-yan<sup>1</sup>  <https://orcid.org/0000-0002-7454-7821>; e-mail: xyli@bnu.edu.cn

\*Corresponding author

<sup>1</sup> State Key Laboratory of Earth Surface Processes and Resource Ecology, Beijing Normal University, Beijing 100875, China

<sup>2</sup> School of Resources and Environmental Engineering, Ludong University, Yantai 264025, China

<sup>3</sup> State Key Laboratory of Loess and Quaternary Geology, Institute of Earth Environment, Chinese Academy of Sciences, Xi'an 710061, China

**Citation:** Cui BL, Li DS, Jiang BF, et al. (2021) Stable isotopes and chloride ion of precipitation events in the northeastern Tibetan Plateau, China. *Journal of Mountain Science* 18(4). <https://doi.org/10.1007/s11629-020-6574-5>

© Science Press, Institute of Mountain Hazards and Environment, CAS and Springer-Verlag GmbH Germany, part of Springer Nature 2021

**Abstract:** Stable isotopes and chloride ion of precipitation are ideal environmental tracers to explain and reveal the formation and evolution mechanisms of water bodies. It is crucial to investigate the stable isotopes and chloride in precipitation events in the northeastern part of the Tibetan Plateau (NETP) due to the limitation of available data. This study sampled each event of precipitation during the period from July 2018 to June 2019 and the monthly dustfall in the NETP to investigate the temporal changes of stable isotopes and chloride in precipitation, and to reveal the moisture source of precipitation over the NETP using a back trajectory model. Results showed that the  $\delta^2\text{H}$  values of precipitation ranged from  $-183.51\%$  to  $17.75\%$ , and the  $\delta^{18}\text{O}$  values ranged from  $-25.18\%$  to  $0.48\%$ . The slope of the Local Meteoric Water Line

was slightly lower than 8 due to the effect of below-cloud secondary evaporation on the precipitation process. Most d-excess values were higher than  $10\%$  because moisture recycled from the continent and Qinghai Lake surface mixed with precipitation. The chloride in precipitation accounted for 86.5% of the annual total deposition mass of chloride ( $1329.64 \text{ mg/m}^2$ ), indicating that precipitation was the main source of chloride in the NETP. The temperature and amount effects of stable isotope in the precipitation were obvious in the NETP. The precipitation was predominantly derived from the Westerly Circulation from September through May and the East Asian Monsoon from June to August, with precipitation amounts of 246.5 mm and 178.0 mm, respectively, indicating that the precipitation over the NETP brought by the Westerly Circulation was more than that brought by the East Asian Monsoon. The air mass over the NETP transited in late May and early

**Received:** 06-Nov-2020

**Revised:** 10-Jan-2021

**Accepted:** 21-Jan-2021

September, and a slight change in transition period would mainly be related to the intensity of the East Asian Monsoon, which is strongly influenced by El Niño-Southern Oscillation. These results provide not only baseline data for hydrological and climatological studies of the NETP but also valuable insights into the hydrological process in the inland arid area of Asia.

**Keywords:** Stable isotope; Chloride ion; Precipitation; Moisture source; Northeastern Tibetan Plateau

## 1 Introduction

Precipitation, the initial source of water for catchments, is a vital component of total fresh water resources on the continent. Especially in inland regions, the ecological ecosystem, industries, and human activities is directly related to precipitation. Stable isotope ( $\delta^2\text{H}$  and  $\delta^{18}\text{O}$ ) in precipitation are ideal environmental tracers for identifying the water sources and hydrological transformation processes, due to the fractionation processes of water isotopes in phase changes (Cai & Tian 2016; Chakraborty et al. 2016; Clark & Fritz 1997; Craig 1961; Dansgaard 1964; Kong et al. 2013; Longinelli et al. 2006; Merlivat & Jouzel 1979). Isotopes are referred to as the “fingerprint” or “DNA” of water because they participate in the entire water circulation process (Clark & Fritz 1997; Gu et al. 2011; Kendall & McDonnell 1998). The compositions of  $\delta^2\text{H}$  and  $\delta^{18}\text{O}$  in local precipitation provide background data for explaining and revealing the formation and evolution mechanism of water bodies, including the moisture source of precipitation, runoff of river water, recharge source and retention times of groundwater, as well as the transport pattern of vadose-zone water (Cui & Li 2015; Mukherjee et al. 2007; Ye & Chang 2019).

Meanwhile, chloride ion in precipitation and atmospheric deposition is also an ideal environmental tracer that obtained wide acceptance and application, due to its strong hydrophilicity and inert nature (Allison & Hughes 1983; Allison et al. 1985; Sharma & Hughes 1985). Chloride ion has been used widely to investigate the water balance assessment, vadose-zone water transport, and the ratio of piston and preferential flow in the vadose zone (Huang et al. 2018; Lu et al. 2020; Scanlon et al. 2007; Xiang et al. 2019). The chloride mass balance method and the chloride accumulation age model have been proposed

to estimate the recharge of precipitation into vadose-zone water and estimate the age of soil water at certain profile depths in the vadose zone, respectively (Allison & Hughes 1983; Sharma & Hughes 1985); these methods have obtained widespread acceptance and application (Huang et al. 2018; Katz et al. 2016; Lu et al. 2020; Scanlon et al. 2006; Xiang et al. 2019; Yidana et al. 2016). This indicates that the investigation of stable isotopes and chloride of precipitation is significant, which is the premise and foundation for exploring the regional water cycle and its transformations (Goni et al. 2001; Negrel et al. 2011).

The Tibetan Plateau (TP), located in central Asia with an average elevation exceeding 4200 m, is known as the earth's “third pole” and the “Asian Water Tower” (Wang et al. 2015; Yanai et al. 1992). It plays important roles not only in the ecological security of China and Asia but also in global climatic change, attracting the extensive attention of scholars, government officials, and international organizations (Bothe et al. 2011; Cai et al. 2017; Zhang et al. 2019). With the research on ice cores in alpine glaciers in the TP, the stable isotopes of precipitation have been studied and focused on in the plateau. The Chinese Academy of Sciences (CAS) launched the Tibetan Plateau Network of Isotopes in Precipitation (TNIP) program to systematically monitor and study the stable isotopes in precipitation and better understand climatic signals conserved in paleo proxies since the 1980s (Yao 2009; Yao et al. 2013). In recent decades, the studies on precipitation isotopes in the TP have made significant progress and led to the publication of high quality research papers. For example, the entire TP was divided into three domains: the monsoon domain, the westerly domain, and the transition domain according to various moisture sources (Yao et al. 2013). Furthermore, the controlling factors on precipitation isotopes were investigated, such as moisture sources, local meteorological conditions, landform, orographic obstacles (Cui & Li 2015; Gao et al. 2018; Ren et al. 2017; Xia et al. 2019; Yang & Yao 2016; Yu et al. 2015, 2016; Zhang et al. 2019; Zhao et al. 2011). However, most of the previous studies have concentrated on the southern and central TP, especially on the monsoon-dominated southern TP (Cai & Tian 2016; Yang et al. 2016; Yao et al. 2013; Zhang et al. 2019).

Furthermore, there are few studies that have investigated the isotopes and chloride in precipitation

to reveal the sources and influential factors of precipitation in the northern part of the TP, especially in the northeastern part of the TP (NETP), due to the limitation of available data (Cui & Li 2015; Yao et al. 2013). For example, there is only one TNIP station settled at Delingha in the vast area of the NETP (Yao et al. 2013). Research on isotopes and chloride in precipitation events in the NETP has not yet been reported and is challenging to conduct. In recent decades, the dramatic changes of surface in the NETP, e.g., grassland degradation, wetland reduction, biodiversity decline, rapid lake expansion, and permafrost melting, have already occurred under the comprehensive influences of human activities and climate change (Cui & Li 2016; Li et al. 2007; Tang et al. 2018; Xin 2008), which have exerted profound influence on the processes of hydrology (Li et al. 2018). Thus, it is crucial to investigate the stable isotopes and chloride in precipitation in the NETP, which would be a significant contribution towards tracing hydrological processes and understanding and managing the local ecology under the changing climate conditions.

Therefore, this study sampled and monitored the precipitation events and the monthly dust fall in the

NETP. The objectives of the study were to (1) investigate the temporal changes of stable isotopes and chloride in precipitation in the NETP, (2) clarify the temperature and precipitation amount effects of stable isotopes in precipitation, and (3) reveal the source of air mass and water moisture over the NETP by using a back trajectory model. The results not only enriched the study of precipitation isotope of the northern TP but also provided baseline data for hydrological and climatological studies in the NETP and will thus, be able to provide valuable insights on the hydrological processes in the alpine environments.

## 2 Materials and Methods

### 2.1 Background of the sampling sites

Sampling sites were set up at the Qinghai Lake Basin (QLB) of the NETP (Fig. 1). The QLB (36°15'–38°20'N, 97°50'–101°20'E), with an area of 29661 km<sup>2</sup>, is a closed basin. It lies in the transitional zone of Westerly Circulation (WC), East Asian Monsoon (EAM), and TP Monsoon (Fig. 1), making the distribution of precipitation and the moisture sources highly complex (Cui & Li 2015; Henderson et al. 2010; Xu et al. 2007). Furthermore, the QLB is an ideal area for studying global climate change, environmental evolution and the uplift process of the TP, as well as the water cycle and eco-hydrological processes, because of its sensitivity to global climate change (An et al. 2012; Cui & Li 2016; Li et al. 2007; Liu et al. 2009).

### 2.2 Sample collection and testing

A precipitation sampling device was deployed at the Meteorological Bureau of Gangcha County (100°08'E, 37°20'N, 3301.5 m) of Qinghai Province, and a dust fall sampling device was

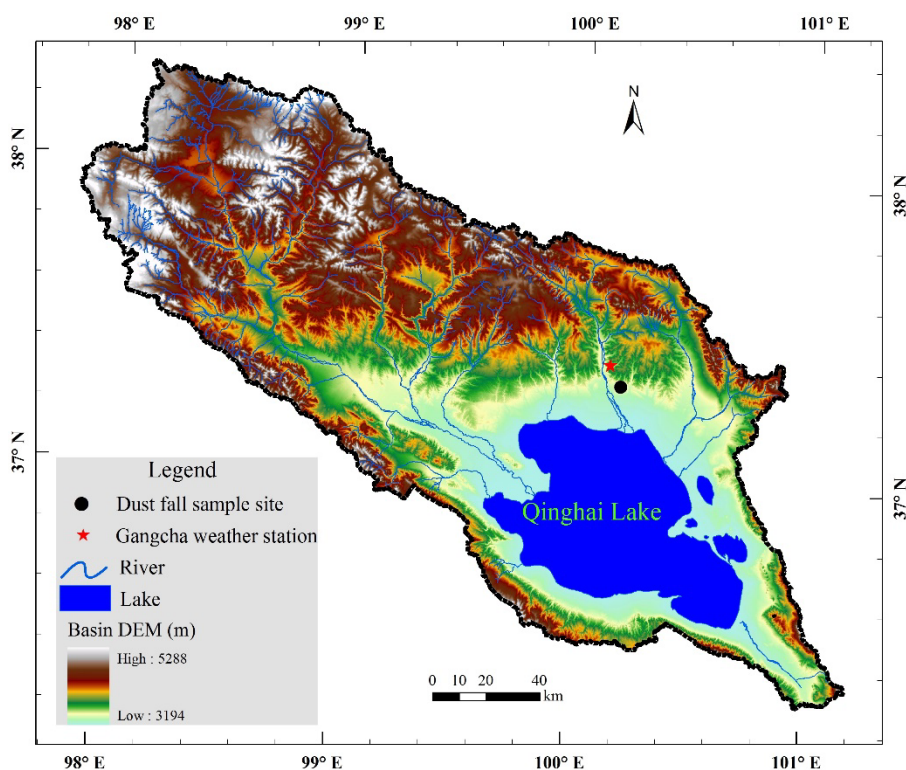


**Fig. 1** Location of the sampling sites for precipitation and dust fall in northeastern part of the Tibetan Plateau.

deployed in the Sanjiaocheng Sheep Farm of Qinghai Province (100°16'E, 37°15'N, 3229.4 m) (Fig. 1). The precipitation samples were collected from every precipitation event during the period from July 2018 to June 2019. If there were more than one precipitation event within a day, each shower was collected as an individual sample. During the sampling period, a total of 136 precipitation samples, including 104 rain, 8 snow, and 24 sleet events, were collected (no precipitation event occurred in December 2018; Fig. 2). Rain samples were taken with a “collector”, composed of a polyethylene tank and a funnel, fitted a ping-pong ball to prevent evaporation of the sample once collected. Snow and sleet samples were collected using a vat installed on the ground and then melted in an airtight container at room temperature. The samples were filtered using 0.45- $\mu\text{m}$  nylon filters and then stored in 30-mL high-density polyethylene bottles. For better interpretation

of the data, precipitation amounts and daily temperatures were also recorded at the station (Fig. 2). The dust fall sampling was performed on a monthly basis, and a total of 12 dust fall samples were collected during the sampling period. 0.03 g of the dust fall sample was taken and washed with 50 mL ultra-pure water in a triangular glass bottle. Then the triangular glass bottle was shaken with a numerical control ultrasonic cleaner for 40 minutes. The dissolved water was filtered using 0.45- $\mu\text{m}$  nylon filters and then stored in 50-mL high-density polyethylene bottles for chloride content testing.

Hydrogen and oxygen stable isotope values ( $\delta^2\text{H}$  and  $\delta^{18}\text{O}$ , respectively) of precipitation were measured using a Los Gatos Research liquid water isotope Analyzer (IWA-45-EP). The measurement accuracy of  $\delta^2\text{H}$  and  $\delta^{18}\text{O}$  values was  $\pm 0.5$  and  $\pm 0.1\%$ , respectively. The chloride content of precipitation and dust fall was measured at Ludong University using ion chromatography (Dionex 600) and the repeated sampling error was 0.5%–1% ( $2\sigma$ ).

### 2.3 Analytical methods

Temperature and precipitation amount effect have been used to assess the effects of environmental changes on the isotopes ( $\delta^2\text{H}$  and  $\delta^{18}\text{O}$ ) of precipitation in the NETP. The temperature effect is a marked positive correlation between the stable isotopic ratio in precipitation and temperature, arises from the fact that the temperature controls the fractionation rate of stable isotopes during phase changes among the solid, liquid, and gaseous phases of precipitation (Dansgaard 1964; Merlivat & Jouzel 1979; Rozanski et al. 1992; Xie et al. 2011). The precipitation amount effect is a marked negative

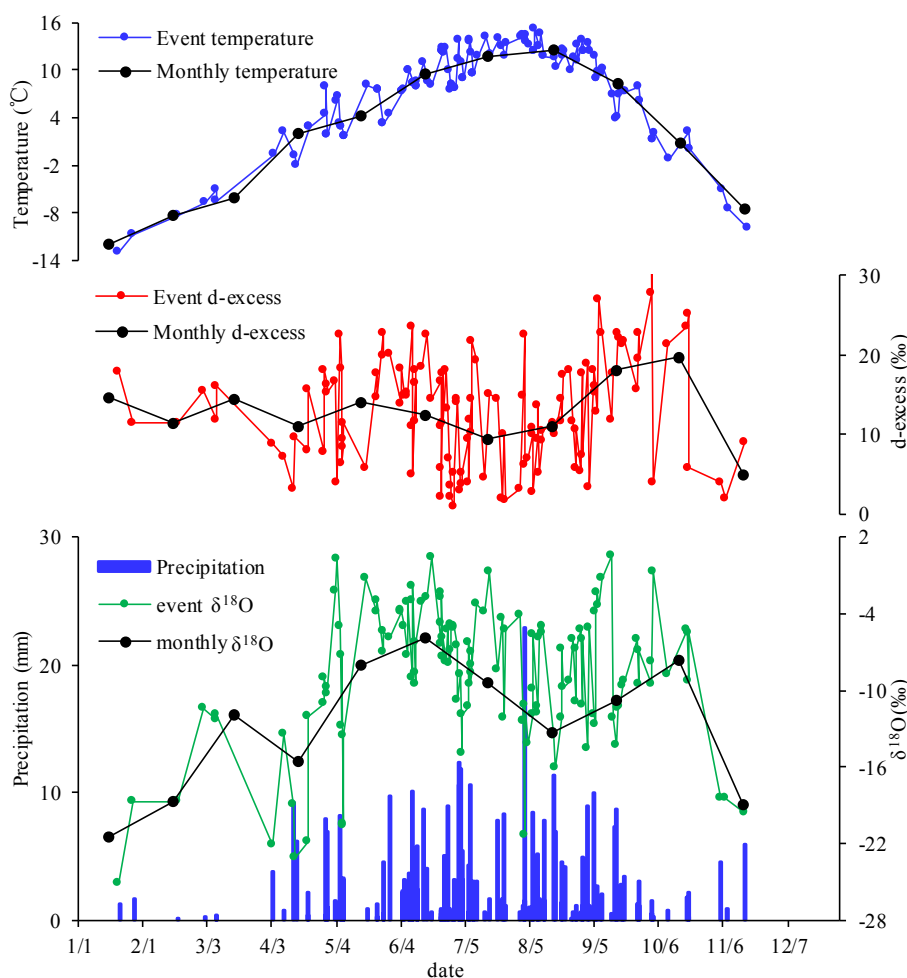


**Fig. 2**  $\delta^{18}\text{O}$ , d-excess and amount of each precipitation event and corresponding temperature during the sampling period. Months from January to June belong to the year 2019. Months from July to December belong to the year 2018.



correlation between precipitation  $\delta^{18}\text{O}$  and amount (Araguás-Araguás et al. 1998; Dansgaard 1964; Xie et al. 2011).

In order to detect the transport paths and moisture sources of precipitation and dust fall, the Hybrid Single-Particle Lagrangian Integrated Trajectory model (HYSPPLIT) was used to perform air mass back trajectory calculations (Stein et al. 2015), which also could reveal the effects of moisture sources and transport patterns on the precipitation  $\delta^{18}\text{O}$  in the NETP. Trajectories, backward to 240 h (10 days), were initiated during the beginnings of each precipitation event. The starting height was determined at 1500 m above ground level (a.g.l) because this height approximates the average height of lifting condensation in the TP (Zhang et al. 2019).

### 3 Results and Discussion

#### 3.1 Characteristics of stable isotope in precipitation events

The  $\delta^2\text{H}$  and  $\delta^{18}\text{O}$  values ranged from -183.51‰ to 17.75‰ and from -25.18‰ to 0.48‰, respectively, with the means of -57.12‰ and -8.69‰, respectively (Fig. 2). Both  $\delta^2\text{H}$  and  $\delta^{18}\text{O}$  values were within the globally reported ranges for precipitation ( $\delta^2\text{H}$ : -350‰–50‰;  $\delta^{18}\text{O}$ : -50‰–10‰) and those across China ( $\delta^2\text{H}$ : -28‰–24‰;  $\delta^{18}\text{O}$ : -35.5‰–2.5‰) (Tian et al. 2001). The range extent was larger than that of the stable isotope values of precipitation in the QLB ( $\delta^2\text{H}$ : -180.80‰–-11.54‰,  $\delta^{18}\text{O}$ : -24.40‰–-2.80‰) due to the different sampling frequencies (Cui & Li 2015). Cui & Li (2015) sampled monthly precipitation, while this study sampled precipitation events. This suggests that precipitation event samples could grasp the characteristics of isotope variation better than monthly or yearly samples. The most negative values generally occurred in January, April and November (Fig. 2).

The plot of  $\delta^2\text{H}$  versus  $\delta^{18}\text{O}$  of precipitation constituted the local meteoric water line (LMWL) (Fig. 3):

$$\delta^2\text{H} = 7.95 \delta^{18}\text{O} + 11.98, \quad (n=136, R=0.99)$$

The LMWL slightly deviated from global meteoric water line (GMWL), which was primarily attributed to the unique local circulation system in the NETP containing different water vapor sources with different evaporation patterns at different spatiotemporal scales (Clark & Fritz 1997; Pang et al.

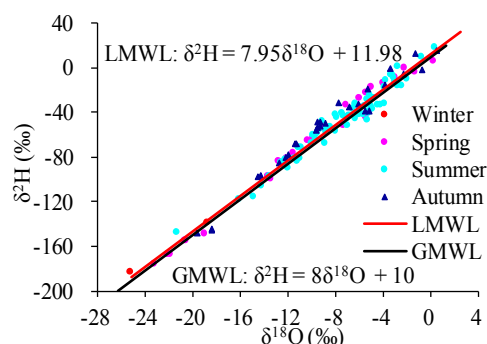


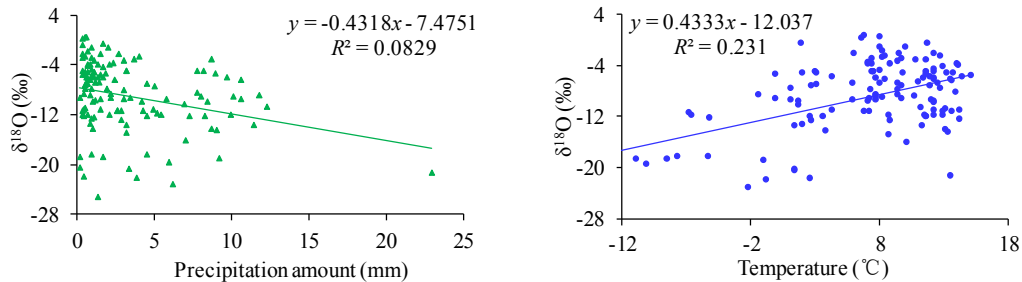
**Fig. 3** The relationship between  $\delta^2\text{H}$  and  $\delta^{18}\text{O}$  of precipitation in the northeastern part of the Tibetan Plateau. LMWL, Local Meteoric Water Line; GMWL, Global Meteoric Water Line.

2017). The LMWL's slope was slightly smaller than that of the global meteoric water line (8), indicating that the precipitation processes in the NETP were affected by below-cloud secondary evaporation. In inland arid areas with low humidity, such as western China with a similar slope of meteoric water lines (7.56; Ma et al. 2009) to this study area, raindrops would undergo evaporation when they fell; this process could cause isotope fractionation in precipitation and consequently, a decrease in the LMWL slope (Araguás-Araguás et al. 1998; Cui & Li 2015; Dansgaard 1964; Zhang & Wang 2016). The similarity of slope between the LMWL and GMWL suggested that the below-cloud evaporation effect was slight in the local precipitation, because the rain formation process occurred under conditions close to isotopic equilibrium (Cui & Li 2015). Froehlich et al. (2008) found that the subcloud evaporation was slight and lower than approximately 1% (nearly free of the subcloud evaporation effect) in Alpine Mountain regions, where the altitude was higher than 1600 m a.s.l. Meanwhile, due to the high d-excess value in local precipitation, the LMWL was slightly above the GMWL (Fig. 2), suggesting that some continental moisture was recycled as the local precipitation (Pang et al. 2017).

The seasonal LMWLs of precipitation were simulated and shown in Table 1. The slope values of the LMWLs in summer and winter seasons were lower than 8, indicating that the precipitation processes in summer and winter seasons were affected by below-cloud secondary evaporation (Dansgaard 1964; Araguás-Araguás et al. 1998; Cui & Li 2015; Zhang & Wang 2016). This would mainly be attributed to relatively low precipitation amount in winter season and relatively high temperature in summer season

**Table 1** The annual and monthly local meteoric water line in the northeastern part of the Tibetan Plateau.

Time period	Equations	<i>n</i>	<i>R</i>	Significant level
Annual	$\delta^2\text{H} = 7.95 \delta^{18}\text{O} + 11.98$	128	0.985	0.001
Spring	$\delta^2\text{H} = 8.24 \delta^{18}\text{O} + 14.96$	27	0.994	0.001
Summer	$\delta^2\text{H} = 7.77 \delta^{18}\text{O} + 9.16$	70	0.980	0.001
Autumn	$\delta^2\text{H} = 8.20 \delta^{18}\text{O} + 18.90$	28	0.984	0.001
Winter	$\delta^2\text{H} = 6.35 \delta^{18}\text{O} - 7.95$	3	1.000	0.019

**Fig. 4** The relationship between precipitation  $\delta^{18}\text{O}$  and corresponding temperature (left) and precipitation amount (right) in the northeastern part of the Tibetan Plateau.

(Figs. 2 and 4), because low precipitation and high temperature both enhance the occurrence of subcloud evaporation. The slope values of LMWLs in spring and autumn seasons were higher than 8 (Table 1), and the isotopic points were mostly located on the upper of the GMWL (Fig. 3), suggesting that the d-excess values of precipitation in spring and autumn seasons were higher than 10‰. The reason should be the moisture derived from the evaporated vapor (Bowen et al. 2012).

Generally, seasonal changes of d-excess in precipitation could be used to investigate the climatic changes of the moisture source regions (Petit et al. 1991), because d-excess value in precipitation is mainly controlled by temperature, wind speed and humidity over the evaporating surface at the moisture source region (Froehlich et al. 2002). According to Fig. 2, the values of d-excess ranged from 0.85‰ to 30.45‰ (average of 12.91‰). Most of the d-excess in monthly precipitation event were all higher than 10‰ (Fig. 4), excluding July (9.34‰) and November (4.95‰). The high d-excess in precipitation would be caused by the large amount of vapor evaporated from the continent and water surface mixing with the precipitation moisture (Fig. 1). The phenomenon was also found in the regions around the Great Lakes, Aral and Caspian Seas, and the eastern Mediterranean (Aizen et al. 1996; Gat & Carmi 1970; Gat et al. 1994; Kreutz et al. 2003). Based on a two-component mixing model, Cui & Li (2015) showed that there was about 23.42% of annual precipitation in the QLB derived from the Qinghai Lake surface evaporation. In this study, the

high d-excess in precipitation also showed that the influences of lakes' evaporation on the atmospheric precipitation and moisture could not be ignored in the NETP. Meanwhile, the changing ranges of  $\delta^{18}\text{O}$  values and d-excess values in precipitation events were more than 25.66‰ and 29.60‰, respectively, indicating the complexity of moisture sources and recycling in the NETP.

### 3.2 Temperature and amount effects of stable isotope in the precipitation

The  $\delta^{18}\text{O}$  variation of the daily precipitation events coincided with the variations in temperature, high  $\delta^{18}\text{O}$  of precipitation peaks generally corresponded to high temperatures, and significant drops in  $\delta^{18}\text{O}$  generally corresponded to low temperatures (Fig. 2), indicating that the temperature effect of  $\delta^{18}\text{O}$  in precipitation was obvious in the NETP. The correlation and regression equation between  $\delta^{18}\text{O}$  of precipitation and temperature was calculated (Fig. 4, Table 2). The significant relationship between the temperature and  $\delta^{18}\text{O}$  in annual precipitation indicated that the temperature effect controlled the  $\delta^{18}\text{O}$  level present in precipitation (Fig. 4). The temperature effect generally appeared in middle-high-latitude inland regions, such as the precipitation in Zhangye, Wulumuqi, Delingha, and other inland areas in central Asia (Tian et al. 2003; Tian et al. 2007; Yao et al. 2013; Yu et al. 2008; Zhang et al. 1995). This would be due to that the continental moisture recycling over the land surface

**Table 2** Temperature effect and amount effect on  $\delta^{18}\text{O}$  of precipitation in the NETP

Effect type	Time period	Equations	<i>n</i>	<i>R</i>	Significant level
Temperature effect	Annual	$\delta^{18}\text{O} = 0.433 T - 12.04$	128	0.481	0.001
	Spring	$\delta^{18}\text{O} = 0.955 T - 13.13$	27	0.565	0.002
	Summer	$\delta^{18}\text{O} = -0.375 T - 3.34$	70	-0.216	0.073
	Autumn	$\delta^{18}\text{O} = 0.443 T - 10.94$	28	0.485	0.009
	Winter	$\delta^{18}\text{O} = 1.363 T - 6.29$	3	0.860	0.341
Amount effect	Annual	$\delta^{18}\text{O} = -0.432 P - 7.48$	128	-0.288	0.001
	Spring	$\delta^{18}\text{O} = -0.286 P - 10.15$	27	-0.131	0.514
	Summer	$\delta^{18}\text{O} = -0.479 P - 5.79$	70	-0.501	0.001
	Autumn	$\delta^{18}\text{O} = -1.047 P - 5.96$	28	-0.550	0.002
	Winter	$\delta^{18}\text{O} = -1.24 P - 19.58$	3	-0.260	0.832

was significant, which could enrich the  $\delta^{18}\text{O}$  in precipitation with relatively high temperatures (Dansgaard 1964; Merlivat & Jouzel 1979; Xie et al. 2011). For example, the  $\delta^{18}\text{O}$  value was amplified by 15% at Delingha due to continental recycling (Yao et al. 2013). Meanwhile, the slope of the temperature effect equation in the NETP (0.43‰/°C) was lower than that at Delingha (0.62‰/°C) which was dominated by WC, while the slope was higher than that at Tuotuohe (0.23‰/°C) which was in the intersection of the shifting influences between Indian monsoon and WC (Yao et al. 2013). According to Table 2, the  $\delta^{18}\text{O}$  values of precipitation were positively and significantly correlated with temperature in spring and autumn seasons ( $P < 0.009$ ). While, the  $\delta^{18}\text{O}$  values were negatively correlated with air temperature in summer precipitation; this would be attributed to the moisture predominantly derived from the EAM from June to August (Cui & Li 2015). This phenomenon is evident in South and East Asia prevailed by a monsoonal climate (Cai et al. 2017).

As shown in Fig. 2 and Fig. 4, high  $\delta^{18}\text{O}$  values of precipitation peaks generally corresponded to low precipitation amounts; conversely, significant drops in  $\delta^{18}\text{O}$  generally corresponded to high precipitation amounts. The  $\delta^{18}\text{O}$  of precipitation was negatively correlated with precipitation amount in precipitation events, with a significance level of 0.001 (Table 2), suggesting that the precipitation amount effect for  $\delta^{18}\text{O}$  in annual precipitation was significant. The slope of the precipitation amount effect equation in the NETP (0.43‰/mm) was higher than that at Delingha (0.01‰/mm) (Yao et al. 2013). In seasonal precipitation, the  $\delta^{18}\text{O}$  values were negatively correlated with precipitation amounts in all seasons, with a significance level of 0.002 in summer and autumn (Table 2). The relationship between  $\delta^{18}\text{O}$  and precipitation amount was relatively complex, the

higher  $\delta^{18}\text{O}$  values concurred with low precipitation amount in winter season when the WC prevails (Yao et al. 2013). Meanwhile, the amount effect is generally observed in tropics and regions affected by marine climates (Xie et al. 2011; Yao et al. 2013). Therefore, the negative correlation between precipitation amount and  $\delta^{18}\text{O}$  of precipitation would be attributed to the moisture predominantly derived from the EAM from June to August (Cui & Li 2015).

Yao et al. (2013) investigated and revealed that the temperature effect of  $\delta^{18}\text{O}$  in precipitation was significant at Delingha, dominated by WC throughout the year, was significant in winter and summer. However, the precipitation  $\delta^{18}\text{O}$  in this study was negatively correlated with temperature in summer (Table 2). This would be attributed to the moisture source of precipitation in the NETP, where the EAM was mainly dominated during the summer season (Cui & Li 2015). Meanwhile, the NETP was influenced strongly by the vapor evaporated from the Qinghai Lake, which also formed distinct regional climate and water cycle in the region (Cui & Li 2015). These furthermore indicated that the moisture sources in the NETP were relatively complex.

### 3.3 Characteristics of chloride in atmospheric deposition

The monthly mass of dust fall samples varied from 2.71 to 64.16 g/m<sup>2</sup> (Fig. 5). The highest deposition occurred in summer, the second highest in early autumn, and the lowest in winter (Fig. 5). The total mass of atmospheric deposition was 279.35 g/m<sup>2</sup> for the whole year, which was similar to that of dust fall collected around Qinghai Lake (265.7 ± 55.0 g/m<sup>2</sup>; 242.5 g/m<sup>2</sup>) by Wan et al. (2012) and Qi et al. (2018), respectively, and a region in Delingha (278.7 g/m<sup>2</sup>) by Gao et al. (2013). Dissolution testing revealed that the annual and monthly deposition masses of chloride

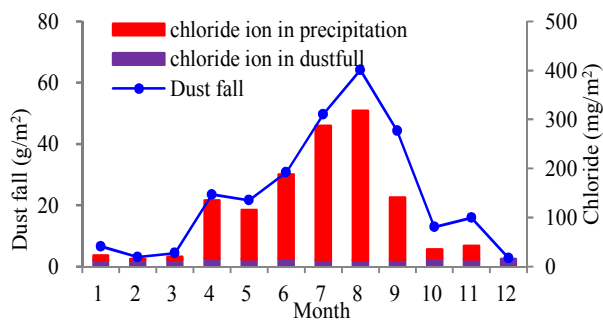


**Fig. 5** Monthly atmospheric deposition masses of dust fall and chloride in the northeastern part of the Tibetan Plateau. Months from January to June belong to the year 2019. Months from July to December belong to the year 2018.

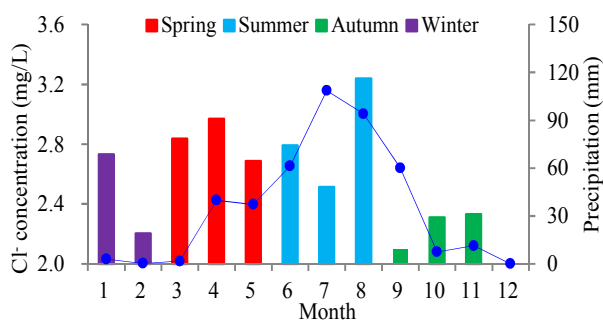


**Fig. 6** Chloride concentration of monthly precipitation and monthly precipitation in the northeastern part of the Tibetan Plateau. Months from January to June belong to the year 2019. Months from July to December belong to the year 2018.

were 1329.64 mg/m<sup>2</sup> and 14.56–317.97 mg/m<sup>2</sup>, respectively (Fig. 5). Chloride mass in atmospheric deposition showed a similar monthly trend as that of the dust fall samples throughout the year, i.e., the deposition gradually increased from January to August and decreased from August to December.

As shown in Fig. 6, monthly chloride concentrations in precipitation ranged from 2.10 to 3.24 mg/L, with a mean of 2.61 mg/L. The values fell within the ranges reported previously for the precipitation around the Qinghai Lake, which ranged from 0.44 to 3.77 mg/L (Jin et al. 2010). The seasonal average chloride concentration in precipitation was in the order: spring > summer > winter > autumn, with values of 2.85 mg/L, 2.80 mg/L, 2.47 mg/L, and 2.25 mg/L, respectively. The monthly deposition mass of chloride in precipitation was calculated and was shown in Fig. 5. The values ranged from 0.44 to 304.96 mg/m<sup>2</sup> and showed seasonal variations: gradually increasing from January to August and then decreasing from August to December. This trend was consistent with the trend of monthly precipitation

amount, indicating that the deposition amount of chloride in precipitation was mainly determined by the precipitation amount (Figs. 5 and 6). Meanwhile, the monthly deposition mass of chloride in dust fall was 13.00–17.79 mg/m<sup>2</sup>, and it showed little variation, being lower in summer and higher in other seasons (Fig. 5).

During the period from October through March with low precipitation (23.5mm; Fig. 6), the chloride deposition mass in dust fall, accounting for 61.5% of the total deposition mass of chloride, was greater than that in precipitation. The chloride deposition mass in precipitation, accounting for 92.4% of the total deposition mass of chloride, was much greater than that in dust fall during the period from April to September (Fig. 5), due to relatively higher precipitation in the period (401mm). The total deposition mass of chloride throughout the year consisted of deposition masses of 1149.70 mg/m<sup>2</sup> and 179.94 mg/m<sup>2</sup> in precipitation and dust fall, respectively. Precipitation chloride accounted for 86.5% of the annual total deposition mass of chloride (Fig. 5), indicating that precipitation was the main source of chloride ions in atmospheric deposition in the NETP. The area surrounding the QLB in the NETP is sparsely populated, with few mineral exploitation activities and factories (Wan et al. 2012). Therefore, the deposition of dust fall and chloride in the NETP mainly originated from the dust carried by airflow, chloride carried by water vapor masses, and locally generated dust.

### 3.4 Sources of atmospheric moisture and deposition

Yao et al. (2013) established a database of precipitation  $\delta^{18}\text{O}$  and used different models to evaluate the climatic controls of precipitation  $\delta^{18}\text{O}$  over the TP. The results showed that Delingha, representing the northern Tibetan Plateau, is hardly influenced by the Indian monsoon (Yao et al. 2013). While, the latitude of the sites in this study (Gangcha; 37°20'N) is similar to that of Delingha (37°22'N), suggesting that the NETP is also hardly influenced by the Indian monsoon. Cui & Li (2015) analyzed the moisture sources of the QLB by using monthly stable isotope of precipitation, showing that the moisture in the basin was predominantly derived from the EAM during the period from June to August and from the WC during the period from September through May.



In this study, the temperature and precipitation amount effects of  $\delta^{18}\text{O}$  in annual precipitation were all significant at a level of 0.001 (Table 2), while the  $\delta^{18}\text{O}$  of precipitation was negatively correlated with air temperature in summer season, and most d-excess values in each precipitation event or monthly precipitation were higher than 10‰ (Figs. 2 and 4). These confirmed the earlier studies indicating that the moisture in the NETP was predominantly derived from the EAM and the WC, and the NETP was influenced strongly by the vapor evaporated from the Qinghai Lake, which also formed distinct regional climate and water cycle in the region (Cui & Li 2015).

The trajectories, backward to 10 days at 1500m a.g.l, of 136 precipitation events were calculated using the HYSPLIT model and was shown in Fig. 7 and Table 3. According to Fig. 7, most air parcels of precipitation over the NETP arrived from the west and east directions, by the WC and EAM, respectively.

During the period from July 2018 to June 2019, there were 87 and 49 precipitation events arriving from the west direction and east direction, respectively, with respective precipitation amounts of 246.5 mm and 178 mm, accounting for 58.07% and 41.93% of annual precipitation, respectively (Table 3), indicating that the precipitation over the NETP brought by the WC was more than that brought by the EAM.

During the period from September to May (dry season), most of the precipitation events (57 events), amounting to 144.6 mm and more than 90% of the total precipitation, were derived from the WC, while three events were derived from the EAM (Table 3), indicating that the moisture was predominantly derived from the WC in dry season; this is in agreement with the results of previous studies (Cui & Li 2015; Yu et al. 2008). This is mainly because a relatively high pressure ridge is formed at 80°–90°E over the TP, leading to the dry and cold air migrates

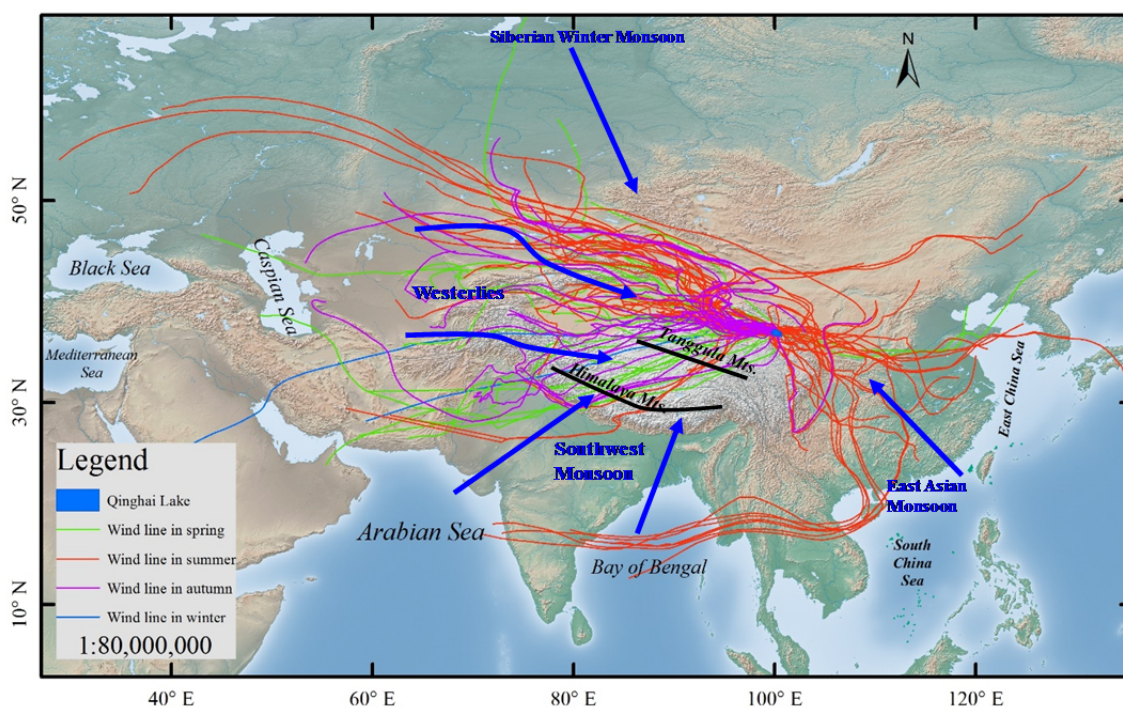


**Fig. 7** The back trajectories of air mass for precipitation events in the northeastern part of the Tibetan Plateau during the period from July 2018 to June 2019.

**Table 3** Quantity and amount of precipitation (Precip.) arrived from Westerly Circulation (WC) and East Asian Monsoon (EAM). n.d. means no data.

Period		Month											Sum
		1	2	3	4	5	6	7	8	9	10	11	
WC	Events (n)	2	1	4	12	11	16	10	4	17	7	3	87
	Precip. (mm)	3.0	0.2	1.6	39.8	30.2	38.3	48.7	14.9	51.1	7.4	11.3	246.5
EAM	Events (n)	n.d.	n.d.	n.d.	n.d.	3	11	10	23	2	n.d.	n.d.	49
	Precip. (mm)	n.d.	n.d.	n.d.	n.d.	7.0	23.0	59.9	79.1	9.0	n.d.	n.d.	178.0

from the TP to the south, east, and north (Araguás-Araguás et al. 1998).

In summer (June to August), there were 30 and 44 precipitation events with precipitation amounts of 101.9 mm and 162.0 mm, respectively, which were derived from the WC and the EAM, respectively (Table 3, Fig. 7), indicating that the precipitation events and amount were predominantly controlled by the EAM in summer. This is mainly attributed to a relatively low pressure center formed at 70°–80°E over the TP, which induces a supply of moist air mass from the Pacific and Indian Oceans to the Asian continent in summer, resulting in relatively high humidity and precipitation over the TP.

According to the Table 3 and Fig. 7, there were several air parcels of precipitation in May and September arriving from the east direction brought by the EAM (3 events on May 26<sup>th</sup> and 29<sup>th</sup>; 2 events on September 1<sup>st</sup> and 2<sup>nd</sup>), suggesting that the transitions of atmospheric circulation over the NETP take place in late May and early September, with the EAM gradually strengthening and the WC gradually weakening in late May, and inversely in early September (Fig. 7; Cui & Li 2015; Gao 1952). Based on the reanalysis data sets from NCEP-NCAR, Cui & Li (2015) showed that the transitions of atmospheric circulation took place in June and September, similar to that in this study (late May and early September, respectively). The slight difference in transition periods would mainly be related to the intensity of the EAM, which is strongly influenced by El Niño-Southern Oscillation (ENSO) (Chen et al. 2018; Xu et al. 2018; Ye et al. 1958). When the period of thermal conversion between East Asian and Western Pacific Ocean is early (late), the EAM could be established early (late) and retreat late (early) and the duration of the EAM is relative long (short), indicating that the onset time of the EAM and the time of thermal conversion between the East Asian and Western Pacific Ocean are consistent (Xu et al. 2018). Cai et al. (2017) contrasted the  $\delta^{18}\text{O}$  values of the ASM precipitation during the La Niña and El Niño years, and their results showed that the  $\delta^{18}\text{O}$  values of the ASM precipitation were positively correlated with ENSO (e.g., high  $\delta^{18}\text{O}$  values corresponding to warm phases).

Fig. 7 showed that there were 12 air masses arriving from the coastal region of Arabian Sea and crossing the Himalayas to reach the study site. Nevertheless, the vapor evaporated from the Arabian

Sea could not reach the NETP due to the long transport distance from the sea and the interception by the Himalayas and Tanggula Mountain, which should enhance upstream convections along the trajectory leading to more condensation of vapor (Cui & Li 2015; Zhang et al. 2019). Meanwhile, all d-excess values of the 12 events was higher than 10‰ ( $> 14.4\%$ ), indicating that the moisture of precipitation was dominated by the continental moisture evaporated along the moisture transport paths (Cai & Tian 2016; Cai et al. 2017). Further, the results of air mass paths and d-excess suggested that the NETP was not influenced by the moisture evaporated from the Indian Ocean (the Arabian Sea and the Bay of Bengal).

According to the Table 3, the precipitation derived from the EAM was 23 mm, 59.9 mm, and 79.1 mm in June, July, and August, respectively, indicating that the influence of EAM on the precipitation over the NETP gradually strengthened from June to August (Araguás-Araguás et al. 1998). Furthermore, there were 30 precipitation events that were derived from the WC in the summer (Table 3, Fig. 7), suggesting that precipitation events should better reflect the moisture source than monthly precipitation (Cai & Tian 2016; Cai et al. 2017; Zhang et al. 2019). It is difficult to distinguish the contributions of WC and EAM based on monthly precipitation, leading to an overestimation of the contribution of the EAM on the precipitation over the NETP (Cui & Li 2015).

Most of the natural dust fall comes from arid and semi-arid regions, where large quantities of loose sediment are located on the surface, which are easily carried aloft by air currents and involved in the global material cycle (Ginoux et al. 2012; Prospero et al. 2002). According the back trajectories of air mass (Fig. 7), the atmospheric deposition in the NETP was mainly carried by the WC originating from the Qaidam Basin, Zhunger Basin, Tarim Basin and arid regions of central Asia, along with the EAM originating from the loess plateau of China. The atmospheric deposition mass of dust fall and chloride in summer were higher than that in the other seasons (Fig. 5). There could be two possible reasons: 1) wind speed is relatively low in summer (Cui & Li 2016), and the atmospheric deposition falls easily under the action of gravity; and 2) precipitation amount is relatively high in summer (Fig. 6), and dust fall acts as a "condensation nucleus", falling with the precipitation (Gong et al. 2012; Kaufman et al. 2005).

Conversely, atmospheric deposition is difficult due to relatively high wind speed and low precipitation amount in other seasons (Cui & Li 2016).

#### 4 Conclusion

Owing to the low humidity, the precipitation process over the NETP was slightly affected by below-cloud secondary evaporation. The temperature and precipitation amount effects of  $\delta^{18}\text{O}$  of annual precipitation were obvious and significant in the NETP. The  $\delta^{18}\text{O}$  value was negatively correlated with air temperature and precipitation in summer precipitation, due to the moisture predominantly derived from the EAM in summer.

The highest deposition occurred in summer, the second highest in early autumn, and the lowest in winter. From October through March, the chloride deposition mass in dust fall (61.5%) was greater than that in precipitation, while the chloride deposition mass in precipitation (92.4%) was much greater than that in dust fall from April to September. Precipitation chloride accounted for 86.5% of the annual total deposition mass of chloride, indicating that precipitation was the main source of chloride in the NETP. The atmospheric deposition in the NETP was mainly facilitated by the WC originating from the Qaidam Basin, Zhunger Basin, Tarim Basin and arid regions of central Asia, along with the EAM

originating from the loess plateau of China.

The moisture was predominantly derived from the WC in dry season (September through May), while the precipitation moisture was predominantly controlled by the EAM in wet season (June to August). The transitions of atmospheric circulation over the NETP take place in late May and early September, and the slight change in transition periods would be mainly related to the intensity of the EAM, which is strongly influenced by ENSO. The precipitation moisture of the NETP was not influenced by the moisture evaporated from the Indian Ocean due to the long transport distance from the sea and the interception by the Himalayas and Tanggula Mountain.

#### Acknowledgements

The study was supported by the National Natural Science Foundation of China (Grant Nos.41877157, 41730854), the State Key Laboratory of Loess and Quaternary Geology (SKLLQG1904), the Science and Technology Support Plan for Youth Innovation of Colleges and Universities of Shandong (2019KJH009), the Natural Science Foundation of Shandong Province (ZR2019MD040) and the State Key Laboratory of Earth Surface Processes and Resource Ecology (2017-KF-15).

#### References

- Aizen V, Aizen E, Melack J, et al. (1996) Isotopic measurements of precipitation on central Asian glaciers (southeastern Tibet, northern Himalayas, central Tien Shan). *J Geophys Res* 101(D4): 9185-9196. <https://doi.org/10.1029/96JD00061>
- Allison GB, Hughes MW (1983) The use of natural tracers as indicators of soil-water movement in a temperate semi-arid region. *J Hydrol* 60(1): 157-173. [https://doi.org/10.1016/0022-1694\(83\)90019-7](https://doi.org/10.1016/0022-1694(83)90019-7)
- Allison GB, Stone WJ, Hughes MW (1985) Recharge in karst and dune element of a semi-arid landscape as indicated by natural isotope and chloride. *J Hydrol* 76(1-2): 1-25. [https://doi.org/10.1016/0022-1694\(85\)90088-5](https://doi.org/10.1016/0022-1694(85)90088-5)
- An ZS, Colman SM, Zhou WJ, et al. (2012) Interplay between the Westerlies and Asian monsoon recorded in Lake Qinghai sediments since 32 ka. *Sci Rep* 2: 619. <https://doi.org/10.1038/srep00619>
- Araguás-Araguás L, Froehlich K, Rozanski K (1998) Stable isotope composition of precipitation over southeast Asia. *J Geophys Res* 103(22): 28721-28742. <https://doi.org/10.1029/98JD02582>
- Bothe O, Fraedrich K, Zhu XH (2011) Large-scale circulations and Tibetan Plateau summer drought and wetness in a high resolution climate model. *Int J Climatol* 31(6): 832-846. <https://doi.org/10.1002/joc.2124>
- Bowen GJ, Kennedy CD, Henne PD, et al. (2012) Footprint of recycled water subsidies downwind of Lake Michigan. *Ecosphere* 3(6): 1-16. <https://doi.org/10.1890/ES12-00062.1>
- Cai Z, Tian L (2016) Atmospheric controls on seasonal and interannual variations in the precipitation isotope in the East Asian Monsoon region. *J Clim* 29(4): 1339-1352. <https://doi.org/10.1175/JCLI-D-15-0363.1>
- Cai ZY, Tian LD, Bowen GJ (2017) ENSO variability reflected in precipitation oxygen isotopes across the Asian Summer Monsoon region. *Earth Planet Sci Lett* 475: 25-33. <https://doi.org/10.1016/j.epsl.2017.06.035>
- Chakraborty S, Sinha N, Chattopadhyay R, et al. (2016) Atmospheric controls on the precipitation isotopes over the Andaman Islands, Bay of Bengal. *Sci Rep* 6: 19555. <https://doi.org/10.1038/srep19555>
- Chen W, Ding SY, Feng J, et al. (2018) Progress in the study of impacts of different types of ENSO on the East Asian monsoon and their mechanisms. *Chin J Atmos Sci* 42(3): 640-655. (in Chinese)
- Clark ID, Fritz P (1997) *Environmental isotopes in hydrogeology*. New York: Lewis Publishers.
- Craig H (1961) Isotopic variation in meteoric waters. *Science* 133(346): 1702-1703. <https://doi.org/10.1126/science.133.3465.1702>
- Cui BL, Li XY (2015) Stable isotope reveal sources of precipitation in the Qinghai Lake Basin of the northeastern Tibetan Plateau. *Sci*



- Total Environ 527: 26-37.  
<https://doi.org/10.1016/j.scitotenv.2015.04.105>
- Cui BL, Li XY (2016) The impact of climate changes on water level of Qinghai Lake in China over the past 50 years. *Hydrol Res* 47(2): 532-542. <https://doi.org/10.2166/nh.2015.237>
- Dansgaard W (1964) Stable isotopes in precipitation. *Tellus* 16(4): 436-468. <https://doi.org/10.3402/tellusa.v16i4.8993>
- Froehlich K, Gibson JJ, Aggarwal PK (2002) Deuterium excess in precipitation and its climatological significance. *Study of Environmental Change using Isotope Techniques*, IAEA, Vienna 54-66.
- Froehlich K, Kralik M, Papesch W, et al. (2008) Deuterium excess in precipitation of Alpine regions-moisture recycling. *Isot Environ Health Stud* 44(1): 61-70.  
<https://doi.org/10.1080/10256010801887208>
- Gao GS, Song LM, Ma ZT (2013) Temporal-spatial distribution and impact factors of dustfall in Qinghai Province of China. *J Desert Res* 33(4): 1124-1130. (in Chinese)
- Gao J, He Y, Masson-Delmotte V, et al. (2018) ENSO effects on annual variations of summer precipitation stable isotopes in Lhasa, southern Tibetan Plateau. *J Clim* 31(3): 1173-1182.  
<https://doi.org/10.1175/JCLI-D-16-0868.1>
- Gao YX (1952) Analysis of the Westerly Cycle over the China in the winter half year by using the temperature of the troposphere. *Acta Meteorologica Sinica* 1: 48-60. (in Chinese)
- Gat JR, Bowser CJ, Kendall C (1994) The contribution of evaporation from the Great Lakes to the continental atmosphere: estimate based on stable isotope data. *Geophys Res Lett* 21(7): 557-560.  
<https://doi.org/10.1029/94GL00069>
- Gat JR, Carmi I (1970) Evolution of the isotopic composition of atmospheric waters in the Mediterranean Sea area. *J Geophys Res* 75(15): 3039-3048. <https://doi.org/10.1029/JC075i015p03039>
- Ginoux P, Prospero JM, Gill TE, et al. (2012) Global-scale attribution of anthropogenic and natural dust sources and their emission rates based on MODIS Deep Blue aerosol products. *Rev Geophys* 5: RG3005. <https://doi.org/10.1029/2012RG000388>
- Gong SL, Lavoue D, Zhao TL, et al. (2012) GEM-AQ/EC, an on-line global multi-scale chemical weather modelling system: model development and evaluation of global aerosol climatology. *Atmos Chem Phys* 12(17): 8237-8256.  
<https://doi.org/10.5194/acp-12-8237-2012>
- Goni IB, Fellman E, Edmunds WM (2001) Rainfall geochemistry in the Sahel region of northern Nigeria. *Atmos Environ* 35(25): 4331-4339. [https://doi.org/10.1016/S1352-2310\(01\)00099-1](https://doi.org/10.1016/S1352-2310(01)00099-1)
- Gu WZ, Pang ZH, Wang QJ (2011) *Isotope Hydrology*. Beijing: Science Press. (in Chinese)
- Henderson ACG, Holmes JA, Leng MJ (2010) Late Holocene isotope hydrology of Lake Qinghai, NE Tibetan Plateau: effective moisture variability and atmospheric circulation changes. *Quat Sci Rev* 29(17-18): 2215-2223.  
<https://doi.org/10.1016/j.quascirev.2010.05.019>
- Huang Y, Chang QR, Li Z (2018) Land use change impacts on the amount and quality of recharge water in the loess tablelands of China. *Sci Total Environ* 628-629: 443-452.  
<https://doi.org/10.1016/j.scitotenv.2018.02.076>
- Jin ZD, Wang SM, Zhang F, et al. (2010) Weathering, Sr fluxes, and controls on water chemistry in the Lake Qinghai catchment, NE Tibetan Plateau. *Earth Surf Process Landf* 35(9): 1057-1070.  
<https://doi.org/10.1002/esp.1964>
- Johnson KR, Ingram BL (2004) Spatial and temporal variability in the stable isotope systematics of modern precipitation in China: implications for paleoclimate reconstructions. *Earth Planet Sci Lett* 220 (3-4): 365-377.  
[https://doi.org/10.1016/S0012-821X\(04\)00036-6](https://doi.org/10.1016/S0012-821X(04)00036-6)
- Katz BS, Stotler RL, Hirmas D, et al. (2016) Geochemical recharge estimation and the effects of a declining water table. *Vadose Zone J* 15(10): 1-13. <https://doi.org/10.2136/vzj2016.04.0031>
- Kaufman YJ, Koren I, Remer LA, et al. (2005) Dust transport and deposition observed from the Terra-Moderate Resolution Imaging Spectroradiometer (MODIS) spacecraft over the Atlantic Ocean. *J Geophys Res-Atmos* 110(D10): S12.  
<https://doi.org/10.1029/2003JD004436>
- Kendall C, McDonnell JJ (1998) *Isotope Tracers in Catchment Hydrology*. Elsevier, Amsterdam. pp 51-86.
- Kong YL, Pang ZH, Froehlich K (2013) Quantifying recycled moisture fraction in precipitation of an arid region using deuterium excess. *Tellus Ser B-Chem Phys Meteorol* 65: 19251.  
<https://doi.org/10.3402/tellusb.v65i0.19251>
- Kreutz KJ, Wake CP, Aizen VB, et al. (2003) Seasonal deuterium excess in a Tien Shan ice core: influence of moisture transport and recycling in Central Asia. *Geophys. Res Lett* 30(18): 1922.  
<https://doi.org/10.1029/2003GL017896>
- Li XY, Xu HY, Sun YL, et al. (2007) Lake-level change and water balance analysis at Lake Qinghai, west China during recent decades. *Water Resour Manag* 21(9): 1505-1516.  
<https://doi.org/10.1007/s11269-006-9096-1>
- Li XY, Yang XF, Ma YJ, et al. (2018) Qinghai Lake Basin Critical Zone Observatory on the Qinghai-Tibet Plateau. *Vadose Zone J* 17(1): 180069. <https://doi.org/10.2136/vzj2018.04.0069>
- Liu WG, Li XZ, Zhang L, et al. (2009) Evaluation of oxygen isotopes in carbonate as an indicator of lake evolution in arid areas: The modern Qinghai Lake, Qinghai-Tibet Plateau. *Chem Geol* 268(1-2): 126-136. <https://doi.org/10.1016/j.chemgeo.2009.08.004>
- Longinelli A, Anglesio E, Flora O, et al. (2006) Isotopic composition of precipitation in Northern Italy: Reverse effect of anomalous climatic events. *J Hydrol* 329(3-4): 471-476.  
<https://doi.org/10.1016/j.jhydrol.2006.03.002>
- Lu YW, Li HJ, Si BC, et al. (2020) Chloride tracer of the loess unsaturated zone under sub-humid region: A potential proxy recording high-resolution hydroclimate. *Sci Total Environ* 700: 134465. <https://doi.org/10.1016/j.scitotenv.2019.134465>
- LZBCAS (Lanzhou Branch of Chinese Academy of Sciences) (1994) *Evolution of recent environment in Qinghai Lake and its prediction*. Science Press, Beijing (in Chinese).
- Ma J, Ding Z, Edmunds WM, et al. (2009) Limits to recharge of groundwater from Tibetan plateau to the Gobi desert, implications for water management in the mountain front. *J Hydrol* 364(1-2): 128-141. <https://doi.org/10.1016/j.jhydrol.2008.10.010>
- Merlivat L, Jouzel J (1979) Global climatic interpretation of the deuterium-oxygen 18 relationship for precipitation. *J Geophys Res* 84 (NC8): 5029-5033. <https://doi.org/10.1029/jc084i08p05029>
- Mukherjee A, Fryar AE, Rowe HD (2007) Regional-scale stable isotopic signatures of recharge and deep groundwater in the arsenic affected areas of West Bengal, India. *J Hydrol* 334(1-2): 151-161.  
<https://doi.org/10.1016/j.jhydrol.2006.10.004>
- Negrel P, Pauwels H, Dewandel B, et al. (2011) Understanding groundwater systems and their functioning through the study of stable water isotopes in a hard-rock aquifer (Maheshwaram watershed, India). *J Hydrol* 397(1-2): 55-70.  
<https://doi.org/10.1016/j.jhydrol.2010.11.033>
- Pang Z, Kong Y, Froehlich K, et al. (2011) Processes affecting isotopes in precipitation of an arid region. *Tellus Ser B-Chem Phys Meteorol* 63(3): 352-359.  
<https://doi.org/10.1111/j.1600-0889.2011.00532.x>
- Pang ZH, Kong YL, Li J, et al. (2017) An isotopic geoinicator in the hydrological cycle. *Proced Earth Plan Sc* 17: 534-537.  
<https://doi.org/10.1016/j.proeps.2016.12.135>
- Petit JR, White JWC, Young NW, et al. (1991) Deuterium excess in recent Antarctic snow. *J Geophys Res-Atmos* 96 (D3): 5113-5122.  
<https://doi.org/10.1029/90JD02232>
- Prospero JM, Ginoux P, Torres O, et al. (2002) Environmental characterization of global sources of atmospheric soil dust identified with the NIMBUS 7 Total Ozone Mapping Spectrometer (TOMS) absorbing aerosol product. *Rev Geophys* 40(1): 1-31.  
<https://doi.org/10.1029/2000RG000095>
- Qi DL, Zhao QN, Zhao HF, et al. (2018) Temporal and spatial variation characteristics and regional differences of dust fall in Qinghai from 2004 to 2017. *Journal of Arid Meteorology*, 36(6): 927-935. (in Chinese)
- Ren W, Yao T, Xie S (2017) Key drivers controlling the stable isotopes in precipitation on the leeward side of the central Himalayas. *Atmos Res* 189: 134-140. <https://doi.org/10.1016/j.atmosres.2017.01.020>
- Rozanski K, Araguás-Araguás L, Gonfiantini R (1992) Relation between long-term trends of oxygen-18 isotope composition of precipitation and climate. *Science* 258(5084): 981-985.  
<https://doi.org/10.1126/science.258.5084.981>
- Scanlon BR, Keese KE, Flint AL, et al. (2006) Global synthesis of groundwater recharge in semiarid and arid regions. *Hydrol Process*



- 20(15): 3335-3370.  
<https://doi.org/10.1002/hyp.6335>
- Scanlon BR, Reedy RC, Tachovsky JA (2007) Semiarid unsaturated zone chloride profiles: Archives of past land use change impacts on water resources in the southern High Plains, United States. *Water Resour Res* 43(6): W06423.  
<https://doi.org/10.1029/2006WR005769>
- Sharma ML, Hughes MW (1985) Groundwater recharge estimation using chloride, deuterium and oxygen-18 profiles in the deep coastal sands of western Australia. *J Hydrol* 81(1-2): 93-109.  
[https://doi.org/10.1016/0022-1694\(85\)90169-6](https://doi.org/10.1016/0022-1694(85)90169-6)
- Stein AF, Draxler RR, Rolph GD, et al. (2015) NOAA's HYSPLIT atmospheric transport and dispersion modeling system. *Bull Amer Meteorol Soc* 96(12): 2059-2077.  
<https://doi.org/10.1175/BAMS-D-14-00110.1>
- Tang LY, Duan XF, Kong FJ, et al. (2018) Influences of climate change on area variation of Qinghai Lake on Qinghai-Tibetan Plateau since 1980s. *Sci Rep* 8: 7331.  
<https://doi.org/10.1038/s41598-018-25683-3>
- Tian L, Yao T, Sun W, et al. (2001) Relationship between delta D and delta O-18 in precipitation on north and south of the Tibetan Plateau and moisture recycling. *Sci China-Earth Sci* 44(9): 789-796.  
<https://doi.org/10.1007/BF02907091>
- Tian LD, Yao TD, MacClune K, et al. (2007) Stable isotopic variations in west China: a consideration of moisture sources. *J Geophys Res-Atmos* 112(D10): D10112.  
<https://doi.org/10.1029/2006JD007718>
- Tian LD, Yao TD, Schuster PF, et al. (2003) Oxygen-18 concentrations in recent precipitation and ice cores on the Tibetan Plateau. *J Geophys Res-Atmos* 108(9): 1-10.  
<https://doi.org/10.1029/2002JD002173>
- Wan DJ, Jin ZD, Wang YX (2012) Geochemistry of eolian dust and its elemental contribution to Lake Qinghai sediment. *Appl Geochem* 27(8): 1546-1555.  
<https://doi.org/10.1016/j.apgeochem.2012.03.009>
- Wang XM, Ma WY, Lang LL, et al. (2015) Controls on desertification during the early twenty-first century in the Water Tower region of China. *Reg Environ Chang* 15(4): 735-746.  
<https://doi.org/10.1007/s10113-014-0661-5>
- Wei KQ, Lin RF (1994) The influence of the monsoon climate on the isotopic composition of precipitation in China. *Geochimica* 23 (1): 32-41. (in Chinese)
- Xia XH, Li SL, Wang F, et al. (2019) Triple oxygen isotopic evidence for atmospheric nitrate and its application in source identification for river systems in the Qinghai-Tibetan Plateau. *Sci Total Environ* 688: 270-280.  
<https://doi.org/10.1016/j.scitotenv.2019.06.204>
- Xiang W, Si BC, Biswas A, et al. (2019) Quantifying dual recharge mechanisms in deep unsaturated zone of Chinese Loess Plateau using stable isotopes. *Geoderma* 337: 773-781.  
<https://doi.org/10.1016/j.geoderma.2018.10.006>
- Xie LH, Wei GJ, Deng WF, et al. (2011) Daily  $\delta^{18}\text{O}$  and  $\delta\text{D}$  of precipitations from 2007 to 2009 in Guangzhou, South China: Implications for changes of moisture sources. *J Hydrol* 400(3-4): 477-489. <https://doi.org/10.1016/j.jhydrol.2011.02.002>
- Xin H (2008) A green fervor sweeps the Qinghai-Tibetan Plateau. *Science* 321(5889): 633-635.  
<https://doi.org/10.1126/science.321.5889.633>
- Xu H, Hou ZH, Ai L, et al. (2007) Precipitation at Lake Qinghai, NE Qinghai-Tibet Plateau, and its relation to Asian summer monsoons on decadal/interdecadal scales during the past 500 years. *Paleogeogr Paleoclimatol Paleocol* 254(3-4): 541-549.  
<https://doi.org/10.1016/j.palaeo.2007.07.007>
- Xu TT, Fan GZ, Zhang YL, et al. (2018) The impact of the thermal differences over the East Asian and the Pacific Ocean on East Asian Monsoon. *Plateau Meteorology* 37(6): 1643-1654. (in Chinese)
- Yanai M, Li C, Song Z (1992) Seasonal heating of the Tibetan Plateau and its effects on the evolution of the Asian summer monsoon. *J Meteorol Soc Jpn* 70(1B): 319-351.  
[https://doi.org/10.2151/jmsj1965.70.1B\\_319](https://doi.org/10.2151/jmsj1965.70.1B_319)
- Yang H, Johnson KR, Griffiths ML, et al. (2016) Interannual con-trols on oxygen isotope variability in Asian monsoon precipitation and im-plications for paleoclimate reconstructions. *J Geophys Res-Atmos* 121(14): 8410-8428.  
<https://doi.org/10.1002/2015JD024683>
- Yang K, Koike T, Fujii H, et al. (2004) The daytime evolution of the atmospheric boundary layer and convection over the Tibetan Plateau: observations and simulations. *J Meteorol Soc Jpn* 82(6): 1777-1792. <https://doi.org/10.2151/jmsj.82.1777>
- Yang X, Yao T (2016) Different sub-monsoon signals in stable oxygen isotope in daily precipitation to the northeast of the Tibetan Plateau. *Tellus Ser B-Chem Phys Meteorol* 68: 27922.  
<https://doi.org/10.3402/tellusb.v68.27922>
- Yao TD (2009) Topic: study on stable isotopes in water of the Qinghai-Tibet Plateau. *Chin Sci Bull* 54(15): 2123. (in Chinese)
- Yao TD, Masson-Delmotte V, Gao J, et al. (2013) A review of climatic controls on  $\delta^{18}\text{O}$  in precipitation over the Tibetan Plateau: Observations and simulations. *Rev Geophys* 51(4): 525-548.  
<https://doi.org/10.1002/rog.20023>
- Ye DZ, Tao SY, Li MC (1958) The mutation phenomenon of the atmospheric circulation in June and October. *Acta Meteorologica Sinica* 29(4): 249-263 (in Chinese).
- Ye RZ, Chang J (2019) Study of groundwater in permafrost regions of China: status and process. *J Glaciol Geocryol* 41(1): 183-196. (in Chinese)
- Yidana SM, Fynn OF, Adomako D, et al. (2016) Estimation of evapotranspiration losses in the vadose zone using stable isotopes and chloride mass balance method. *Environ Earth Sci* 75(3): 208.  
<https://doi.org/10.1007/s12665-015-4982-6>
- Yu W, Tian L, Ma Y, et al. (2015) Simultaneous monitoring of stable oxygen isotope composition in water vapour and precipitation over the central Tibetan Plateau. *Atmos Chem Phys* 15(18): 10251-10262.  
<https://doi.org/10251-10262.10.5194/acp-15-10251-2015>
- Yu W, Wei F, Ma Y, et al. (2016) Stable isotope variations in precipitation over Deqin on the southeastern margin of the Tibetan Plateau during different seasons related to various meteorological factors and moisture sources. *Atmos Res* 170: 123-130.  
<https://doi.org/10.1016/j.atmosres.2015.11.013>
- Yu WS, Yao TD, Tian LD, et al. (2008) Relationships between  $\delta^{18}\text{O}$  in precipitation and air temperature and moisture origin on a south-north transect of the Tibetan Plateau. *Atmos Res* 87(2): 158-169.  
<https://doi.org/10.1016/j.atmosres.2007.08.004>
- Zhang MJ, Wang SJ (2016) A review of precipitation isotope studies in China: basic pattern and hydrological process. *J Geogr Sci* 26(7): 921-938. <https://doi.org/10.1007/s11442-016-1307-y>
- Zhang T, Zhang YS, Guo YH, et al. (2019) Controls of stable isotopes in precipitation on the central Tibetan Plateau: A seasonal perspective. *Quat Int* 513: 66-79.  
<https://doi.org/10.1016/j.quaint.2019.03.031>
- Zhang XP, Yao TD (1995) Relations between weather systems affecting Tibetan Plateau and oxygen isotope in precipitation. *J Glaciol Geocryol* 17(2): 125-131 (in Chinese).
- Zhao L, Yin L, Xiao H, et al. (2011) Isotopic evidence for the moisture origin and composition of surface runoff in the headwaters of the Heihe River basin. *Chin Sci Bull* 56(4-5): 406-415.  
<https://doi.org/10.1007/s11434-010-4278-x>